

Three-Electron Auger Process from Beam-Foil Excited Multiply Charged Ions

Enrico De Filippo,¹ Gaetano Lanzanò,¹ Hermann Rothard,^{2,*} and Claude Volant³

¹*INFN Sezione di Catania, Via Santa Sofia 64, 95123 Catania, Italy*

²*Centre de Recherche sur les Ions, les Matériaux et la Photonique,
(CEA/CNRS UMR 6252/ENSICAEN/Université de Caen Basse Normandie),
CIMAP-CIRIL-Ganil, BP 5133, 14070 Caen Cedex 05, France*

³*DAPNIA/SPhN, CEA/Saclay, F-91191 Gif-sur-Yvette Cedex, France*

(Received 29 January 2008; revised manuscript received 4 April 2008; published 13 June 2008)

Electron emission from collisions of C^{3+} ions (22.7 A MeV) with carbon foils (21, 49 and 90 $\mu\text{g}/\text{cm}^2$) was studied by the time-of-flight method. Two prominent emission patterns can be readily identified as “binary encounter” electrons and “cusp” electrons. With the thinnest target only, a third structure is visible at slightly lower time-of-flight (thus slightly higher energy) than the cusp electrons. The energy of these electrons would correspond to 647_{-104}^{+116} eV if they were emitted from the projectile frame of reference. A possible explanation is a rare three-electron-Auger $K^2L^2L^1$ process.

DOI: 10.1103/PhysRevLett.100.233202

PACS numbers: 34.50.Fa, 79.20.-m

The radiationless deexcitation of atoms with an inner shell vacancy was discovered experimentally by and named after Pierre Auger. In this nowadays well understood process, a vacancy in an inner shell X is filled by an electron from an outer shell Y . The energy is transmitted to a second electron (from a shell Z). The most common Auger transitions are of the type XYX (KLL , LMM , etc.). Another important class is formed by the “Coster-Kronig” transition XXY (such as, e.g., LLM). Furthermore, if, for example, the K shell is doubly ionized, and the L shell filled, hypersatellite Auger lines K^2LL are observed at higher energies than the K^1LL Auger lines with one K -shell vacancy. Auger electron emission is an alternative deexcitation channel in concurrence to characteristic x-ray emission, where a photon is emitted instead of an electron. An important feature of both characteristic x rays and Auger electrons is that their final energy is determined by the electron binding energies in the atom. Therefore, the measurement of energy spectra of x-ray and Auger lines induced by γ , x-ray, electron, proton, or heavy ion irradiation of samples have become important means of materials analysis. For example, *target* Auger electron spectroscopy is the standard method of surface analysis. In collisions involving “dressed” heavy ions, which carry at least two electrons, also the in-flight emission of Auger electrons from the excited *projectile* can be observed [1,2]. This is a complex process, since the projectiles must be “prepared” in a configuration allowing an Auger transition to occur: at least one inner shell vacancy and at least two electrons in an outer shell must be present.

In addition to the above-mentioned two-electron Auger (or one-electron one-photon) processes, also another fundamental Auger process, involving three electrons (or two electrons and one photon) is conceivable when two inner shell vacancies and at least three outer shell electrons are present. If, for example, the K shell is empty, and three electrons are located in the L shell, two of the three L -shell

electrons “simultaneously” transit to the K shell and transmit the gained energy to the *one* single electron left in the L shell ($K^2L^2L^1$ transition). One way to prepare such “hollow atoms” (or, in some cases “hollow ions”), is via target electron capture to outer shells (a “feeding of excited projectile states” from the reservoir of target electrons) of slow highly charged ions approaching a surface. This was shown experimentally by Moretto-Capelle *et al.* [3] and Folkerts *et al.* [4]. Another possibility is the formation of inner shell vacancies with non-negligible probability of producing two inner shell vacancies (in the percent range) in ion-atom collisions with nearly symmetric collision systems as first reported by Afrosimov *et al.* [5]. Also, the corresponding two-electron one-photon emission process was discovered experimentally at the same time [6]. These studies triggered several theoretical investigations (see [7,8], and references therein) for low- Z ions. More recently, also high- Z ions were investigated theoretically [9], and upper cross section limits for the time-reversal process of the three-electron Auger process, the “trielecronic recombination” were obtained with a channeling technique [10]. These rare three-electron processes are of fundamental interest for the study of three-electron correlation in bound systems [10], they are forbidden in independent particle models like Hartree-Fock and become allowed only in the many-body approach [7–9].

Vacuum conditions and surface contamination may be a problem for such rare processes (the branching ratio of $K^2L^2L^1$ to KLL transition is of the order of 10^{-4} [4,5,7–9]) in slow ion collisions since not only *projectile*- but also *target* Auger emission in the energy range in question ($E < 1000$ eV) is possible [4,5]. Here, we report on a different way to prepare the ion configuration leading to $K^2L^2L^1$ transition, i.e., beam-foil excitation, where a swift ion beam interacts with a thin foil. Auger electron emission from the fast *projectile* takes place with energies in the laboratory frame well above 10 000 eV so that it is impos-

sible that *target* Auger electrons could obscure the spectra. The experiment was performed with a beam of C^{3+} (22.7A MeV) traversing thin carbon foils (thickness 21, 49, and 90 $\mu\text{g}/\text{cm}^2$) at the superconducting cyclotron CS at LNS (Catania) in the large scattering chamber CICLOPE with the ARGOS multidetector [11,12]. Fast scintillation detectors of the “phoswich” type (a BaF_2 crystal covered with a plastic scintillation foil mounted on a photomultiplier tube) allow identifying ionic particles (protons, deuterons, heavy ions), neutrons, energetic photons (γ or x rays) and electrons. The velocity of the particle can be measured by the time-of-flight method since the ion beams delivered by the cyclotron are pulsed with a small pulse width of typically below 1 ns and the distance between target and detector (typically about 1–4 m) can be measured with great precision. For about the past ten years, ARGOS, initially designed for studying nuclear heavy ion reactions [11], was used to measure electron emission in atomic collisions [12]. This detection system has several advantages compared to electrostatic or magnetic electron spectrometers such as accurate measurement of absolute cross sections, the possibility to study electron-electron coincidences, and an important “dynamics” concerning the measurement of doubly differential yields. The doubly differential spectra measured with ARGOS extend over up to 6 orders of magnitude [13].

During an experiment aimed at a systematic study of electron emission as a function of a (projectile-target) matrix (C,Ni,Au-C,Ni,Au) at fixed projectile velocity of $\sim 23\text{A MeV}$ [13], we used a special monitoring detector mounted at a very large distance from the target (~ 4 m, thus having an excellent resolution) at an observation angle of $\theta = 10^\circ$. Furthermore, this detector also had a very low detection threshold. It was always running as general control monitor (normalization, beam intensity) in parallel to all (single or grouped) runs with other detectors. Therefore, the data taken with this detector also have a very high count number (excellent statistics). In this way, quasi “accidentally,” we discovered a spectral feature which can only be interpreted as evidence for a $K^2L^2L^1$ transition. Experimental data obtained with the special detector at $\theta = 10^\circ$ with C^{3+} at 22.7A MeV are shown in Figs. 1 and 2. The fast scintillator signal, which is proportional to the electron energy, is plotted as a function of the electron time-of-flight for the thinnest carbon target of 21 $\mu\text{g}/\text{cm}^2$ in Fig. 1. Such a bidimensional plot allows in a more clear-cut way than simple “spectra” to observe and identify specific structures and emission patterns. Doubly differential electron yields as a function of the electron time-of-flight for three different thin carbon foils (thickness 21, 49, and 90 $\mu\text{g}/\text{cm}^2$) are compared in Fig. 2.

The first structure (highest energy, shortest time-of-flight) belongs to “binary encounter” electrons (BEE). This basic ionization process is rather well understood: target electrons are scattered by the projectile’s Coulomb

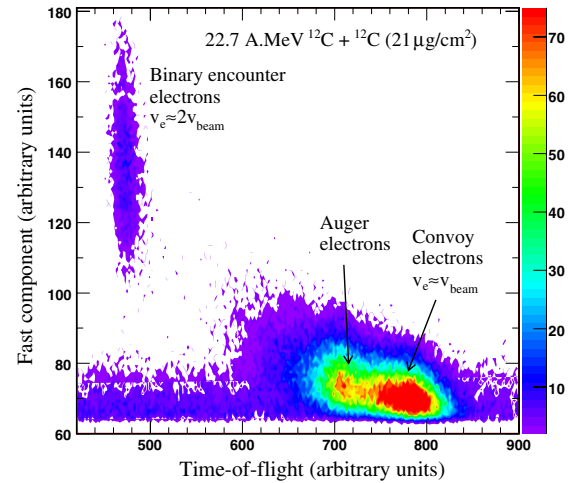


FIG. 1 (color online). The fast scintillator signal (proportional to the electron energy) as a function of the electron time-of-flight for the collision system 22.7A MeV C^{3+} on C foil (21 $\mu\text{g}/\text{cm}^2$). The observation angle is $\theta_{\text{lab}} = 10^\circ$.

field. As can be seen in Fig. 2, BEE give rise to a distinct peak at an electron velocity of about twice the projectile velocity $v_{\text{BEE}} \approx 2v_{\text{beam}}$ at small laboratory angles θ . The peak width is determined by the Compton profile of the bound target electrons and the resolution of the spectrometer. For thin enough targets, the single differential yield

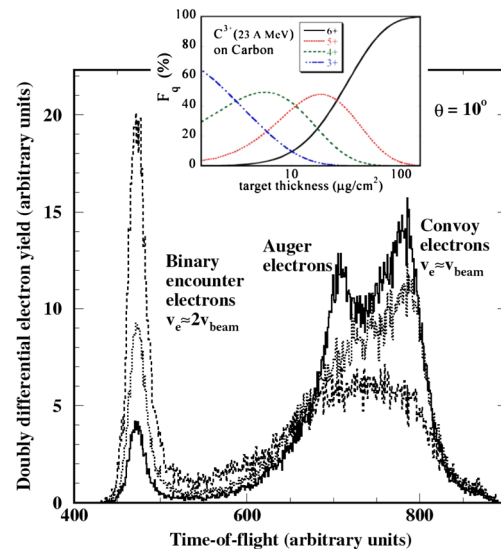


FIG. 2 (color online). Doubly differential electron yields as a function of the electron time-of-flight recorded at an observation angle of $\theta_{\text{lab}} = 10^\circ$ with a beam of C^{3+} (22.7A MeV) traversing three different thin carbon targets (thickness 21, 49, and 90 $\mu\text{g}/\text{cm}^2$, solid, dotted, and dashed histograms, respectively). The spectra are normalized to the number of incoming ions. The inset shows the evolution of the outgoing charge state fractions F_q ($q = 3+, 4+, 5+, 6+$) as a function of carbon target thickness for the incoming C^{3+} (23A MeV) beam calculated with the ETACHA code [20].

(i.e., the peak area) is proportional to the target thickness. The most prominent structure appears at a larger time of flight (lower energy) near an electron velocity approximately equal to the projectile velocity $v_{\text{cusp}} \approx v_{\text{beam}}$. These so-called “cusp” or “convoy” electrons are produced by electron transfer to projectile continuum states. In single collisions, electron capture to continuum of target electrons or projectile electron loss to continuum (ELC) contribute. In solids, depending on the target thickness, a dynamical equilibrium correlated to the evolution of the ion charge state fractions and including the possibility of multistep processes (capture to bound states followed by ELC) is reached (see Fig. 2). In the present case (ELC dominating), the cusp peak decreases with target thickness, since less projectile electrons are available because of increasing stripping. We refer the reader to [12–14] for a detailed discussion of production mechanisms of electrons in fast atomic collisions.

With the thinnest target only, a third structure is visible at slightly lower time-of-flight (thus slightly higher energy) than the cusp electrons [15]. The energy of these electrons would correspond to 647_{-104}^{+116} eV if they were emitted from the projectile [17]. Since numerical values for peak positions and widths have been determined in the time-of-flight spectra, conversion into energy values leads to asymmetric error bars. A possible—and for the present time the only conceivable—explanation for the peak observed at $v_{\text{lab}} = 7.32$ cm/ns is the above-mentioned three-electron-Auger $K^2L^2L^1$ process, which has been observed in collisions of slow multiply charged carbon ions capturing electrons and deexciting in front of a solid surface at an energy of 592 eV with a full width at half maximum (FWHM) of 40 eV [4]. In our case, the FWHM is found to be 79 eV. This value is mainly determined by the broadening expected from the time resolution of our measurement caused by the width of the ion pulse. Therefore, since we are at the limit of the time resolution of the present experiment, the only careful conclusion we can draw here is that the measured linewidths of the two different experiments are not incompatible. We note that the carbon K^1LL peak (one K vacancy) can be observed at an energy of about 260 eV, and the hypersatellite K^2LL peak (two K vacancies) at about 315 eV when emitted from a solid carbon target or a free carbon projectile [4,19]. Auger emission is isotropic in the projectile frame of reference. Therefore, from velocity vector addition follows that at a fixed observation angle, two Auger lines can be observed at the high-velocity side and the low-velocity side of the so-called cusp or convoy electron peak in the laboratory system [1,2]. The latter peak cannot be seen in Figs. 1 and 2 since it falls just below the detection limit of the scintillators. It is interesting to note that projectile Auger electron emission can be viewed as “in-flight fragmentation of the atomic system” and bears strong similarities to light charged particle emission from the highly

excited projectilelike system in nuclear collisions: an interesting analogy in nuclear physics is the observation of two peaks of projectile fragments around the projectile velocity [11].

The three-electron Auger process can take place only in a configuration where three electrons are present in the L shell while the K shell is empty. In the present case, the incoming C^{3+} projectile has 3 bound electrons. The inset in Fig. 2 shows the calculated evolution of the charge state fractions F_q for incoming C^{3+} as a function of the C target thickness for the charge states $q = 3+, 4+, 5+,$ and $6+$. The calculation was made with the PC-based numerical simulation “ETACHA” developed by Rozet *et al.* [20] which was shown to reproduce the measured preequilibrium charge state distributions quite well for fast few electron ions in the energy range from approximately 10 to 80A MeV [20,21]. The initial charge state $q = 3$ rapidly vanishes and is extinct above $35 \mu\text{g}/\text{cm}^2$. Indeed, with the thicker targets of 49 and $90 \mu\text{g}/\text{cm}^2$ the observed peak structure disappears since less than three electrons are left in bound states of the projectile. For targets thicker than $120 \mu\text{g}/\text{cm}^2$ the ion is nearly completely stripped. Electron capture is extremely unlikely for high velocity low- Z_p ions. This means that here the population of the L shell is due to collisional excitation from the K shell to the L shell. We note that also excitation from the L shell to the M shell leading to LMM Auger emission with incoming Ni^{19+} where only the K and L shell are initially populated was found [18].

The yield of the Auger electrons is comparable to that of the BEE at 10° , the absolute production cross section is of the order of ≈ 20 kb/sr. Unfortunately, we cannot give the branching ratio of $K^2L^2L^1$ to KLL transition and compare them to the data of Folkerts *et al.* [4], since the KLL peak, which can only be observed up to a limiting emission angle of $\theta = 5^\circ$, is merged with the convoy electron peak and with the detectors used at such small angles cannot clearly be separated. In the data taken at $\theta_{\text{lab}} = 10^\circ$ shown in Figs. 1 and 2, only the transition at about 600 eV can be seen for kinematical reasons [1,2,18]. This may, however, be achieved in future dedicated experiments with the measurement of a complete angular distribution with small angular steps, better time-of-flight resolution, and by carefully “preparing” the ion configuration via the target thickness dependence of the ion configuration. The observation of such rare processes [3–9] is possible only under particular experimental conditions such as highly charged ions plus electron capture at surfaces [4], channeling [10], or, as in the present case, a beam-foil method combined with a powerful detector. This latter method opens the door to detailed studies of the dynamics and complex mechanisms of the electron excitation process inside a solid which are not yet quantitatively understood.

We would like to thank all our collaborators (in particular S. Hagmann). Special thanks to the LNS-CS staff for

providing excellent ion beams. Thanks to N. Giudice, N. Guardone, V. Sparti, and S. Urso from INFN Sez. Catania, V. Campagna, G. De Luca, A. Di Stefano, and A. Salomone from INFN-LNS for technical assistance and to C. Marchetta, and E. Costa for target preparation. Two of us (H.R. and C.V.) would like to thank their Sicilian colleagues for their great hospitality and INFN for financial support.

*Corresponding author.

rothard@ganil.fr

- [1] N. Stolterfoth, Phys. Rep. **146**, 315 (1987).
- [2] G. Lanzaò, E. De Filippo, S. Hagmann, H. Rothard, and C. Volant, Nucl. Instrum. Methods Phys. Res., Sect. B **256**, 510 (2007).
- [3] P. Moretto-Capelle, A. Bordenave-Montesquieu, P. Benoit-Cattin, S. Andriamonje, and H. J. Andrä, Z. Phys. D **21**, S347 (1991).
- [4] L. Folkerts, J. Das, S. W. Bergsma, and R. Morgenstern, Phys. Lett. A **163**, 73 (1992).
- [5] V. V. Afrosimov, Yu. S. Gordeev, A. N. Zinov'ev, D. Kh. Rasulov, and A. P. Shergin, Zh. Eksp. Teor. Fiz. Pis. Red. **21**, 535 (1975) [JETP Lett. **21**, 249 (1975)].
- [6] W. Wölfl, Ch. Stoller, G. Bonani, M. Suter, and M. Stöckli, Phys. Rev. Lett. **35**, 656 (1975).
- [7] M. Y. Amusia and I. S. Lee, J. Phys. B **24**, 2617 (1991).
- [8] N. Vaeck and J. E. Hansen, J. Phys. B **25**, 3613 (1992).
- [9] J. P. Marques, F. Parente, P. Indelicato, and J. P. Desclaux, J. Phys. B **31**, 2897 (1998).
- [10] M. Chevallier, C. Cohen, N. Cue, D. Dauvergne, J. Dural, P. Gangnan, R. Kirsch, A. L'Hoir, D. Lelièvre, J.-F. Libin, P. H. Mokler, J.-C. Poizat, H.-T. Prinz, J.-M. Ramillon, J. Remillieux, P. Roussel-Chomaz, J.-P. Rozet, F. Sanuy, D. Schmaus, C. Stephan, M. Toulemonde, D. Vernhet, and A. Warczak, Phys. Rev. A **61**, 022724 (2000).
- [11] G. Lanzaò, E. De Filippo, M. Geraci, A. Pagano, S. Aiello, A. Cunsolo, R. Fonte, A. Foti, M. L. Sperduto, C. Volant, J. L. Charvet, R. Dayras, and R. Legrain, Nucl. Phys. A **683**, 566 (2001).
- [12] E. De Filippo, G. Lanzaò, and H. Rothard, Nucl. Phys. News **17**, 24 (2007).
- [13] E. De Filippo, G. Lanzaò, H. Rothard, C. Volant, A. Anzalone, N. Arena, M. Geraci, F. Giustolisi, and A. Pagano, Eur. Phys. J. A **32**, 349 (2007).
- [14] H. Rothard and B. Gervais in *Ion Beam Science—Solved and Unsolved Problems*, edited by Peter Sigmund [Mat. Fys. Medd. Dan. Vid. Selsk. **52**, 497 (2006)].
- [15] Besides BEE, cusp, and Auger electrons, a closer inspection of the data shown in Figs. 1 and 2 shows also evidence for electrons with velocities in-between that of the cusp electrons and the BEE. The velocity of these electrons extends in the laboratory system up to almost 9–10 cm/ns, corresponding to 25–31 keV. Complex dynamic mechanisms as described in [16] may explain their origin.
- [16] D. C. Ionescu and A. Belkacem, Eur. Phys. J. D **18**, 301 (2002).
- [17] This value is obtained as follows: First, in the relative time-of-flight spectra of Fig. 2, an exponential function was fitted to the “background” given by the cusp peak, and a Gaussian distribution was fitted to the superposed Auger peak. The uncertainty of the Gaussian peak position c_{Auger} is estimated to be within 1 TDC (time to digital converter) channel. Then the relative time-of-flight scale (in TDC channels c) was converted into an absolute time scale $t(\text{ns}) = a(c - c_0)$, where the TDC conversion constant was found to be $a = 0.0936$ ns/channel for the 10° detector. a [ns/channel] was obtained by a linear fit on the time-values given by a precise time calibrator as a function of different delay times (from 10 to 200 ns in steps of 10 ns). The “physical” time-of-flight starts at the offset (or “zero-time”) channel c_0 and can be obtained from the relation $t_{\text{known}}(\text{ns}) = a(c_e - c_0)$. Here, t_{known} is a reference time and c_e the corresponding channel in the electron time-of-flight spectrum. We have used $t_{\text{known}} = t_{\text{BEE}} = d/v_{\text{BEE}}$, where $d = 398.2$ cm is the distance of the detector from the target and $v_{\text{BEE}} = 12.25$ cm/ns is the expected velocity for BE electrons emitted at 10° . The position of the BEE peak, c_{BEE} as obtained by fitting the experimental peak by a Gaussian distribution is estimated to be reliable within 1 channel. Assuming an uncertainty of 1° in the angular position of the detector, we obtain $c_0 = 149 \pm 2$ TDC channels. In principle, c_0 can also be determined from t_{cusp} or $t_{\text{X-rays}}$. However, for this particular collision system (C on C), there are no high energy x rays, and the low energy side of the cusp electron peak ($v_{\text{beam}} = 6.5$ cm/ns, $E_{\text{cusp}} = 12.3$ keV) may be affected in part by detection threshold effects as discussed in [13]. This calibration procedure yields $v_{\text{Auger lab}} = 7.32 \pm 0.04$ cm/ns at $\theta_{\text{lab}} = 10^\circ \pm 1^\circ$ in the laboratory frame. Finally, inserting $v_{\text{Auger lab}} = 7.32 \pm 0.04$ cm/ns, $v_{\text{beam}} = 6.50$ cm/ns and $\theta_{\text{lab}} = 10^\circ \pm 1^\circ$ in relativistic kinematics formulas for velocity vector addition [18], the electron energy $E_{\text{Auger proj}} = 647_{-104}^{+116}$ eV and emission angle $\theta_{\text{Auger proj}} \sim 61^\circ$ in the projectile frame of reference are found. Uncertainties contributing to the error bars arise mainly from the fitting procedure, the determination of the “zero-time” c_0 in the time-of flight calibration, and the accuracy of the angular position of the detector.
- [18] G. Lanzaò, E. De Filippo, H. Rothard, C. Volant, A. Anzalone, N. Arena, M. Geraci, F. Giustolisi, and A. Pagano, Nucl. Instrum. Methods Phys. Res., Sect. B **233**, 31 (2005).
- [19] M. Caron, H. Rothard, M. Beuve, and B. Gervais, Phys. Scr. **T92**, 281 (2001).
- [20] J. P. Rozet, C. Stéphan, and D. Vernhet, Nucl. Instrum. Methods Phys. Res., Sect. B **107**, 67 (1996).
- [21] H. Rothard, J. P. Grandin, M. Jung, A. Clouvas, J. P. Rozet, and R. Wünsch, Nucl. Instrum. Methods Phys. Res., Sect. B **132**, 359 (1997).